Molecular Geometry and Conformational Stability of 4,5-Dimethyl- and 3,4,5,6-Tetramethylphenanthrene: A Look at the Structural Basis of the Buttressing Effect

Richard N. Armstrong,* Herman L. Ammon,* and John N. Darnow

Contribution from the Department of Chemistry and Biochemistry, University of Maryland, College Park, Maryland 20742. *Received August 18, 1986*

Abstract: The molecular structures and conformational stabilities of 4,5-dimethyl- (**2**) and 3,4,5,6-tetramethylphenanthrene (**3**) have been examined by X-ray crystallography, the temperature dependence of the kinetics of the pseudorotation process, and force-field calculations of the molecular geometries of the ground-state and transition-state structures. Crystal structures of **2** and **3** show the aromatic systems to have the expected helical twist imposed by the methyl groups at the 4- and 5-positions. The angle between the mean planes of the outer rings in **2** of 27.9° is increased to 29.2° in **3** due to the buttressing effect of the methyl groups at the 3- and 6-positions. Force-field calculations with the MMP2 program give good reproductions of the ground-state structures of **2** and **3** and provide heat-of-formation data in reasonable agreement with previously determined experimental values. The strain energy of **2** with respect to phenanthrene, **1**, is calculated to be 10.5 kcal/mol with the methyl groups in the 3- and 6-positions of **3** contributing a buttressing effect of 2.2 kcal/mol, numbers which compare favorably with experimental and corrected experimental values, respectively. Lattice energy calculations suggest the experimental value for the buttressing effect of 7.2 kcal/mol is in error due to an overestimation of $\Delta H°_{sublimation}$ for **3**. The conformational enantiomers of **2** and **3** can be separated by chromatography on (+)-poly(triphenylmethyl methacrylate) coated silica, the former compound being separable only at cryogenic temperatures (−70 to −80 °C). Absolute configurations of the antipodes are deduced by circular dichroism spectroscopy. Activation barriers ($\Delta G^{\ddagger}$) for pseudorotation of **2** and **3** are found to be 16.1 and 23.1 kcal/mol, respectively. Molecular mechanics calculations provide reasonable transition-state structures for **2** and **3** which have activation barriers (17.4 and 23.1 kcal/mol) in good agreement with the experimental measurements. The experimental (or calculated) buttressing effect of the additional methyl groups in **3** in the ground state and in the barrier to pseudorotation are used to estimate a difference in the strain energies of **2** and **3** in the transition state of 8–10 kcal/mol. The structural manifestation of the added methyl groups in the transition state for **3** appears in part as an increase in the in-plane pivoting of the outer rings away from methyl–methyl interaction.

For over 50 years there has been continued interest in relationships between the structure and physical and chemical properties of strained or sterically hindered aromatic hydrocarbons. Several particularly interesting examples of such molecules have been derived from the phenanthrene, **1**, and 9,10-dihydrophenanthrene skeletons, which have alkyl substituents at the 4- and 5-positions or at the 3-, 4-, 5-, and 6-positions. It was pointed out by Newman[1] some time ago that the most likely structural manifestation of strain in molecules of the 4,5-dimethylphenanthrene type was displacement of the methyl groups out of the mean plane of the aromatic system and/or distortion of the aromatic plane. The structural distortion expected in 4,5-dimethylphenanthrenes was subsequently demonstrated[2] by the partial resolution of the antipodes of 4,5,8-trimethyl-1-phenanthrylacetic acid, **4**, chiral by virtue of kinetically stable out-of-plane bending of the methyl groups. Distortion of the aromatic system through twisting of the 4a–4b bond is also evident from the red shift of the L_b transition in the UV spectrum of **2** compared to that of **1** as predicted by molecular orbital calculations.[3] Although molecular mechanics calculations[4,5] suggest substantial deformation of the aromatic plane of **2** occurs, the relative contributions of out-of-plane bending of the methyl groups and distortion of the aromatic rings to the relief of methyl–methyl interactions have not been evaluated experimentally.

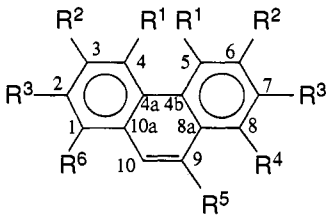

	R^1	R^2	R^3	R^4	R^5	R^6
1	H	H	H	H	H	H
2	CH_3	H	H	H	H	H
3	CH_3	CH_3	H	H	H	H
4	CH_3	CH_3	H	CH_3	H	CO_2H
5	$AcOCH_2$	H	H	H	H	H
6	CH_3	CH_3	H	H	AcO	H
7	H	H	CH_3	H	H	H
8	CH_3	H	CH_3	H	H	H

It is well documented that placement of methyl groups at the 3- and 6-positions (e.g., 3,4,5,6-tetramethylphenanthrene, **3**) increases steric crowding by "buttressing" the methyl groups at the 4- and 5-positions. The "buttressing effect"[6] in **3** was originally observed[7] experimentally through a difference of 7.2 ± 1.4 kcal/mol in the ground-state strain energies of **2** and **3**. The effect was also observed by a further red shift of the L_b transition in the UV spectrum and a shift in the polarographic reduction potential of **3**.[8] A buttressing effect of between 5 and 6 kcal/mol in the barrier to pseudorotation in **3** has been recently estimated[9] from literature values for the activation energies of **5**[10] with those of **3**[11] or **6**.[9] Similarly, a buttressing effect of 5.9 ± 0.7 kcal/mol has been measured in the pseudorotation of the dihydroaromatic *cis*-3,4,5,6-tetramethyl-9,10-dihydroxy-9,10-dihydro-

(1) Newman, M. S. *J. Am. Chem. Soc.* **1940**, *62*, 2295.
(2) Newman, M. S.; Hussey, A. S. *J. Am. Chem. Soc.* **1947**, *69*, 3023.
(3) (a) Cromartie, R. I. T.; Murrell, J. N. *J. Chem. Soc.* **1961**, 2063. (b) Suzuki, H. *Electronic Absorption Spectra and Geometry of Organic Molecules*; Academic Press: New York, 1967; pp 380–383.
(4) Kitaigroodsky, A. I.; Dashevsky, V. G. *Tetrahedron* **1968**, *24*, 5917.
(5) Kao, J.; Allinger, N. L. *J. Am. Chem. Soc.* **1977**, *99*, 975.
(6) Rieger, M.; Westheimer, F. H. *J. Am. Chem. Soc.* **1950**, *72*, 19.
(7) Karnes, H. A.; Kybett, B. D.; Wilson, M. H.; Margrave, J. L.; Newman, M. S. *J. Am. Chem. Soc.* **1965**, *87*, 5554.
(8) Jezorek, J. R.; Mark, H. B. *J. Org. Chem.* **1971**, *36*, 666.
(9) Armstrong, R. N.; Lewis, D. A.; Darnow, J. N.; Ammon, H. L. In *Enzyme Catalyzed Reactions: Stereochemistry*; Frey, P. A., Ed.; Elsevier: New York, 1986; pp 267–280.
(10) Munday, R.; Sutherland, I. O. *J. Chem. Soc. B* **1968**, 80.
(11) Scherubl, H.; Fritzsche, U.; Mannschreck, A. *Chem. Ber.* **1984**, *117*, 336.

0002-7863/87/1509-2077$01.50/0

phenanthrene.[9,12] A small but measurable effect has also been noted in the polarographic reduction potential of the corresponding 9,10-quinones of **2** and **3**.[13]

In as much as no information on the structural geometry of **2** and **3** is available except that obtained from model building or molecular mechanics calculation,[4,5] we report here the results of an X-ray crystallographic investigation of these compounds. Furthermore, we describe the first isolation and direct observation of the conformational antipodes of **2** by HPLC at cryogenic temperatures on a chiral stationary phase. Molecular mechanics calculations with the MMP2 program and Allinger's 1982 force field[14] reproduce good ground-state geometries for **2** and **3** and provide a look at the structure of the transition states for pseudorotation of these molecules. Activation barriers for inversion of configuration of **2** and **3** are found to be in excellent agreement with those predicted by force-field calculation. These observations provide further insight into the structural basis of the "buttressing effect" in both the ground and transition states of **2** and **3**.

Experimental Section

X-ray Crystallography. Samples of **2** and **3** were obtained from Prof. M. S. Newman.[15] X-ray measurements were made on 0.2 × 0.3 × 0.3 mm crystal specimens of **2** and **3** obtained from 90% and 95% ethanol/water, respectively. X-ray data were collected on an Enraf-Nonius CAD-4 diffractometer with Mo radiation (graphite monochromator, Kα λ = 0.71069 Å). Cell parameters were obtained from least-squares refinement of 25 automatically centered Bragg angles. **2**: space group $P2_1$; a = 8.327 (1) Å, b = 8.2540 (8) Å, c = 8.746 (1) Å, β = 107.63 (1)°, Z = 2, ρ_{calcd} = 1.196 g cm^{-3}. **3**: space group $P2_1/c$; a = 11.635 (1) Å, b = 15.417 (1) Å, c = 14.921 (3) Å, β = 90.45 (1)°, Z = 8, ρ_{calcd} = 1.163 g cm^{-3}. Intensity data were determined with the 2θ–ω scan procedure. Each scan was composed of 96 steps, the upper and lower 16 steps of which were used for background. The scan speed was variable and depended upon evaluation of a prescan intensity for each reflection. Six standards were measured every 2 h of X-ray exposure; intensity fluctuation corrections were applied. Automatic reorientation was performed at 1000 reflection intervals. 2θ maximum = 50°. **2**: 1259 data measured; 1157 unique data, 862 $I > 3\sigma(I)$. **3**: 5444 data measured; 4898 unique data; 2618 $I > 3\sigma(I)$. Structures were solved by direct methods. The ring-linked hydrogen positions were calculated; all methyl hydrogens were located from difference maps. Structure refinement was by full matrix least squares with anisotropic temperature factors for carbon and individual isotropic terms for hydrogen and included a correction for secondary extinction. The function minimized was $\sum w(F_o - F_c)^2$, $w = (1/\sigma(F))^2$; only reflections for which $I > 3\sigma(I)$ were included in the refinement. The final R ($\sum||F_o| - |F_c||/\sum|F_o|$) and weighted R ($[\sum w(|F_o| - |F_c|)^2/\sum wF_o^2]^{1/2}$) factors were 0.034, 0.050 for **2** and 0.050, 0.039 for **3**. All crystallographic calculations were performed with the TEXRAY package (Molecular Structure Corp.) on either a Digital Equipment Corp. MicroVax I or II.

Other Calculations. Molecular mechanics computations were done utilizing the program MMP2 and Allinger's 1982 force field.[14] Lattice energies (heats of sublimation) for **2** and **3** were calculated with the WMIN program,[16] which uses a potential of the form

$$V = q_iq_jr_{ij}^{-1} - a_ia_jr_{ij}^{-6} + b_ib_j \exp[-(c_i + c_j)r_{ij}]$$

The various q, a, b, and c coefficients were taken from work on hydrocarbons by Williams and Starr.[17]

Preparation and Stability of Conformational Antipodes. Separation of the conformational enantiomers of **3** was accomplished by chromatography at 0 °C on a 4.6 mm × 25 cm Chiralpak OP(+) column ((+)-poly(triphenylmethyl methacrylate) coated on silica)[18] eluted at 0.56 mL/min with n-hexane (**3M**, k' = 1.18; **3P**, k' = 2.16, α = 1.82) or on microcrystalline triacetylcellulose.[11] Separation of the kinetically labile antipodes of **2** proved considerably more difficult. However, a reasonable separation was achieved on a Chiralpak OP(+) column cooled to −70 to −80 °C with immersion in a slurry of dry ice and 95% ethanol and eluted with n-hexane at 1.0 mL/min (**2M**, k' = 4.44; **2P**, k' = 5.73, α = 1.29). Column backpressure did not exceed 150 bars under these conditions.

Table I. Positional Parameters and B(eq) for 4,5-Dimethylphenanthrene

atom	x	y	z	B(eq)
C1	1.1061 (7)	0.4500	0.5142 (5)	6.0 (2)
C2	1.2694 (8)	0.4104 (7)	0.5480 (5)	6.6 (2)
C3	1.3219 (6)	0.3001 (7)	0.4523 (5)	5.9 (2)
C4	1.2089 (4)	0.2367 (6)	0.3142 (4)	3.9 (1)
C4A	1.0397 (4)	0.2952 (5)	0.2647 (4)	3.5 (1)
C4B	0.9158 (4)	0.2557 (5)	0.1111 (4)	3.5 (1)
C5	0.9503 (4)	0.2249 (5)	−0.0348 (4)	3.7 (1)
C6	0.8230 (5)	0.1716 (6)	−0.1651 (5)	4.8 (2)
C7	0.6592 (6)	0.1549 (7)	−0.1620 (6)	6.3 (2)
C8	0.6171 (5)	0.2059 (7)	−0.0308 (6)	6.0 (2)
C8A	0.7446 (4)	0.2617 (6)	0.1055 (5)	4.6 (2)
C9	0.6945 (6)	0.3392 (7)	0.2323 (7)	6.1 (2)
C10	0.8126 (7)	0.4121 (7)	0.3530 (6)	6.1 (2)
C10A	0.9899 (6)	0.3894	0.3757 (4)	4.7 (2)
C11	1.2671 (6)	0.0920 (7)	0.2422 (6)	4.9 (2)
C12	1.1137 (6)	0.2667 (7)	−0.0651 (5)	5.0 (2)
H1	1.05 (1)	0.53 (1)	0.604 (8)	13 (2)
H2	1.329 (5)	0.459 (6)	0.643 (5)	5.3 (8)
H3	1.441 (4)	0.232 (6)	0.495 (5)	4.8 (8)
H6	0.837 (4)	0.156 (4)	−0.252 (4)	2.6 (7)
H7	0.545 (9)	0.10 (1)	−0.249 (8)	13 (2)
H8	0.506 (9)	0.20 (1)	−0.032 (8)	11 (2)
H9	0.554 (5)	0.346 (7)	0.214 (5)	6 (1)
H10	0.768 (6)	0.476 (7)	0.441 (6)	8 (1)
H11A	1.163 (5)	0.040 (5)	0.161 (5)	5.0 (9)
H11B	1.342 (5)	0.113 (6)	0.195 (5)	6 (1)
H11C	1.342 (5)	0.019 (5)	0.333 (4)	4.4 (8)
H12A	1.207 (5)	0.325 (6)	0.014 (5)	5 (1)
H12B	1.187 (6)	0.166 (7)	−0.095 (5)	7 (1)
H12C	1.084 (5)	0.327 (7)	−0.169 (6)	7 (1)

Samples were collected at −78 °C, and their CD spectra were obtained at −60 °C on a JASCO J-500 C spectropolarimeter. Circular dichroic extinction coefficients ($\Delta\epsilon$) were determined by using concentrations calculated from UV spectra with ϵ_{255} = 43 600 M^{-1} cm^{-1} for **2** and ϵ_{262} = 49 100 for **3**.

A chiral sample of 3,4,5,6-tetramethyl-9-acetoxyphenanthrene (**6M**) was prepared by low-temperature acid-catalyzed dehydration of *cis*-3,4,5,6-tetramethyl-9,10-dihydroxy-9,10-dihydrophenanthrene of known absolute configuration[9,12,19] (3.8 M CF_3CO_2H in CH_2Cl_2, 5 min, −15 °C) followed by trapping of the phenol (acetic anhydride, pyridine, 1 h, −15 °C). ^{1}H NMR (200 MHz, $(CD_3)_2CO$, reference external Me_4Si) δ 2.41 (br s, 3 H), 2.42 (br s, 3 H), 2.43 (s, 3 H), 2.47 (br s, 3 H), 2.48 (br s, 3 H), 7.25 (s, 1 H), 7.42 (d, 1 H, J = 7.8 Hz), 7.45 (d, 1 H, J = 8.2 Hz), 7.60 (d, 1 H, J = 7.9 Hz), 7.69 (d, 1 H, J = 8.1 Hz).

Rate constants and activation parameters for pseudorotation of **3M** and **6M** were derived from the temperature dependence (25 to 55 °C) of the kinetics for disappearance of the circular dichroic transition at 275 nm in n-hexane. Racemization of **2M** was followed at 271 nm between −40 and −70 °C.

Results and Discussion

Solid-State Molecular Geometries. ORTEP representations of **2** and **3** are shown in Figure 1. Atomic coordinates for both structures are listed in Tables I and II, respectively. The carbon–carbon bond distances in the phenanthrene framework of **2** and **3** are quite similar. However, compared to **1** the 4–4A and 1–10A bond distances in **2** and **3** are about 0.02 Å longer and shorter, respectively, than those in **1**. It is clear from Figure 1 as well as the structural features summarized in Table III that steric hindrance between the methyl groups at the 4- and 5-positions imposes a pronounced twist on the aromatic system. In contrast **1** is essentially a planar molecule with a very small (approximately 2°) twist between the mean planes of the two outer rings.[20] Although the buttressing effect of the additional methyl groups at the 3- and 6-positions on the strain and conformational stability of **3** and similar molecules is documented, the structural manifestations of the effect have not been documented. The contact distance of the interior (4 and 5) methyl groups in both **2** and **3** is 2.98 Å. The effect of the additional methyl groups at

(12) Armstrong, R. N.; Lewis, D. A. *J. Org. Chem.* **1985**, *50*, 907.
(13) Karnes, H. A.; Rose, M. L.; Cobalt, J. W.; Newman, M. S. *J. Am. Chem. Soc.* **1968**, *90*, 458.
(14) Allinger, N. L.; Flanagen, H. L. *J. Comput. Chem.* **1983**, *4*, 399.
(15) Newman, M. S.; Lilje, K. C. *J. Org. Chem.* **1979**, *44*, 4944.
(16) Busing, W. R. *Oak Ridge National Laboratory Report 5747*, 1981.
(17) Williams, D. E.; Starr, T. L. *Comput. Chem.* **1977**, *1*, 173.
(18) Okamoto, Y.; Okamoto, I.; Yuki, H.; Murata, S.; Noyori, R.; Takaya, H. *J. Am. Chem. Soc.* **1981**, *103*, 6971.
(19) Armstrong, R. N.; Lewis, D. A.; Ammon, H. L.; Prasad, S. M. *J. Am. Chem. Soc.* **1985**, *107*, 1057.
(20) Kay, M. I.; Okaya, Y.; Cox, D. E. *Acta Crystallogr.* **1971**, *B27*, 26.

Table II. Positional Parameters and B(eq) for 3,4,5,6-Tetramethylphenanthrene

atom	x	y	z	B(eq)
C1	0.2708 (2)	0.1772 (2)	0.4492 (2)	4.4 (2)
C2	0.2871 (3)	0.2515 (2)	0.4966 (2)	4.6 (2)
C3	0.2259 (2)	0.3269 (2)	0.4755 (2)	4.0 (1)
C4	0.1549 (2)	0.3284 (2)	0.3999 (2)	3.5 (1)
C4A	0.1512 (2)	0.2552 (2)	0.3418 (2)	3.2 (1)
C4B	0.0930 (2)	0.2537 (2)	0.2539 (2)	3.3 (1)
C5	0.0836 (2)	0.3263 (2)	0.1952 (2)	3.7 (1)
C6	0.0128 (2)	0.3210 (2)	0.1196 (2)	4.3 (1)
C7	−0.0420 (3)	0.2432 (3)	0.0989 (2)	5.1 (2)
C8	−0.0197 (2)	0.1699 (2)	0.1467 (2)	4.9 (2)
C8A	0.0509 (2)	0.1728 (2)	0.2232 (2)	3.8 (1)
C9	0.0898 (3)	0.0947 (2)	0.2656 (2)	4.5 (2)
C10	0.1681 (3)	0.0970 (2)	0.3313 (2)	4.5 (2)
C10A	0.1997 (2)	0.1768 (2)	0.3731 (2)	3.6 (1)
C11	0.0721 (3)	0.4032 (2)	0.3906 (3)	4.6 (2)
C12	0.1615 (3)	0.4038 (2)	0.2042 (2)	4.5 (2)
C13	0.2366 (4)	0.4040 (3)	0.5363 (3)	5.7 (2)
C14	−0.0003 (4)	0.3975 (3)	0.0574 (3)	6.2 (2)
C1−	−0.5258 (3)	0.3455 (2)	0.1734 (2)	5.1 (2)
C2−	−0.5507 (3)	0.2726 (3)	0.2213 (2)	5.2 (2)
C3−	−0.4953 (2)	0.1946 (2)	0.2020 (2)	4.5 (2)
C4−	−0.4229 (2)	0.1884 (2)	0.1283 (2)	3.6 (1)
C4A−	−0.4113 (2)	0.2603 (2)	0.0694 (2)	3.3 (1)
C4B−	−0.3519 (2)	0.2579 (2)	−0.0168 (2)	3.4 (1)
C5−	−0.3481 (2)	0.1839 (2)	−0.0741 (2)	3.4 (1)
C6−	−0.2735 (2)	0.1832 (2)	−0.1472 (2)	4.0 (1)
C7−	−0.2104 (3)	0.2575 (2)	−0.1665 (2)	5.0 (2)
C8−	−0.2272 (3)	0.3323 (2)	−0.1215 (2)	4.9 (2)
C8A−	−0.3001 (2)	0.3356 (2)	−0.0471 (2)	4.0 (1)
C9−	−0.3317 (3)	0.4159 (2)	−0.0067 (2)	5.1 (2)
C10−	−0.4119 (3)	0.4192 (2)	0.0575 (2)	5.2 (2)
C10A−	−0.4525 (2)	0.3416 (2)	0.0987 (2)	4.0 (1)
C11−	−0.3482 (3)	0.1091 (2)	0.1212 (2)	4.5 (2)
C12−	−0.4352 (3)	0.1117 (2)	−0.0671 (2)	4.2 (2)
C13−	−0.5133 (4)	0.1183 (3)	0.2637 (3)	6.4 (2)
C14−	−0.2629 (4)	0.1048 (3)	−0.2067 (3)	5.6 (2)
H1	0.307 (2)	0.117 (2)	0.468 (2)	5.7 (7)
H2	0.343 (2)	0.252 (2)	0.550 (2)	6.3 (7)
H7	−0.093 (2)	0.240 (2)	0.045 (2)	7.3 (8)
H8	−0.054 (2)	0.108 (2)	0.133 (2)	6.6 (8)
H9	0.068 (2)	0.041 (1)	0.240 (1)	3.1 (5)
H10	0.204 (2)	0.047 (2)	0.358 (2)	4.5 (6)
H11A	0.017 (2)	0.393 (2)	0.343 (2)	4.8 (7)
H11B	0.031 (2)	0.411 (2)	0.448 (2))	8 (1)
H11C	0.110 (2)	0.464 (2)	0.375 (2)	6.7 (8)
H12A	0.220 (2)	0.397 (2)	0.255 (2)	5.2 (7)
H12B	0.119 (2)	0.461 (2)	0.217 (2)	4.9 (7)
H12C	0.210 (2)	0.410 (2)	0.148 (2)	6.8 (8)
H13A	0.296 (3)	0.396 (2)	0.580 (2)	9 (1)
H13B	0.167 (3)	0.423 (2)	0.566 (2)	9 (1)
H13C	0.265 (3)	0.459 (2)	0.501 (2)	10 (1)
H14A	−0.056 (3)	0.383 (2)	0.016 (2)	10 (1)
H14B	−0.032 (4)	0.445 (3)	0.087 (3)	14 (2)
H14C	0.073 (3)	0.415 (2)	0.029 (2)	11 (1)
H1−	−0.551 (2)	0.405 (2)	0.189 (2)	5.1 (7)
H2−	−0.604 (2)	0.279 (2)	0.274 (2)	5.9 (7)
H7−	−0.166 (2)	0.254 (2)	−0.221 (2)	4.4 (6)
H8−	−0.193 (2)	0.387 (2)	−0.138 (2)	4.6 (6)
H9−	−0.299 (2)	0.468 (2)	−0.036 (2)	4.9 (7)
H10−	−0.443 (2)	0.474 (2)	0.081 (2)	6.3 (8)
H11A−	−0.289 (2)	0.117 (1)	0.075 (2)	3.5 (6)
H11B−	−0.392 (2)	0.056 (2)	0.110 (2)	6.2 (8)
H11C−	−0.306 (2)	0.097 (2)	0.183 (2)	5.8 (7)
H12A−	−0.494 (2)	0.123 (2)	−0.017 (2)	5.7 (7)
H12B−	−0.400 (2)	0.052 (2)	−0.054 (2)	6.4 (8)
H12C−	−0.478 (2)	0.104 (2)	−0.129 (2)	6.5 (8)
H13A−	−0.567 (3)	0.134 (2)	0.310 (2)	10 (1)
H13B−	−0.523 (3)	0.063 (3)	0.231 (3)	12 (2)
H13C−	−0.443 (3)	0.101 (2)	0.296 (3)	11 (1)
H14A−	−0.203 (3)	0.115 (2)	−0.246 (2)	8 (1)
H14B−	−0.247 (3)	0.056 (2)	−0.172 (2)	11 (1)
H14C−	−0.335 (3)	0.097 (2)	−0.245 (2)	10 (1)

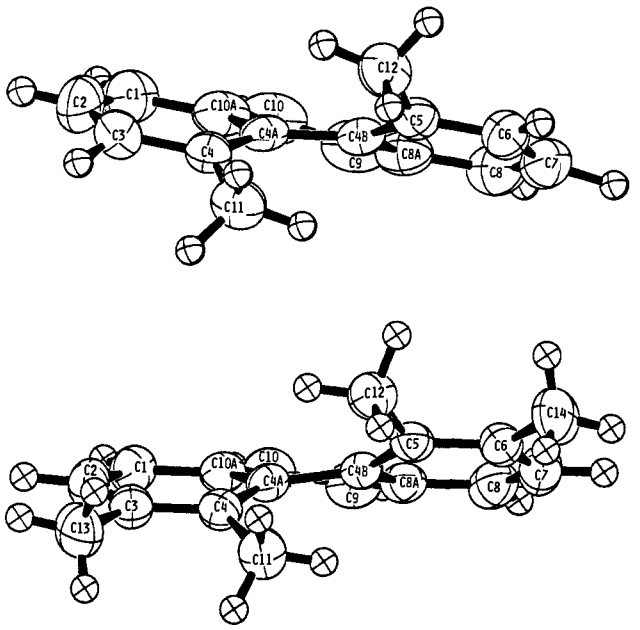

Figure 1. ORTEP drawings of the structures of **2** (top) and **3** (bottom). The carbon atoms are shown as 50% probability ellipsoids and hydrogen atoms as spheres with B = 1.5 Å. Only one of the two independent molecules of **3** in the crystal asymmetric unit is illustrated here. Complete structural inforamtion is given in supplementary material.

Table III. Selected Experimental and Calculated[a] Structural Parameters for **2** and **3**

	2		**3**[b]	
distance (Å) or angle (deg)	exptl	calcd	exptl	calcd
4-4A-4B-5	31.5 (3)	34.6	32.9 (2)	34.9
11-4···5-12[c]	67.4 (4)	74.7	73.3 (4)	78.4
11-4-3-13			11.1 (3)	13.8
angle between mean planes 1-2-3-4-4A-10A and 4B-5-6-7-8-8A	27.9 (1)	29.4	29.2 (1)	30.1
displacement of 11 from 1-2-3-4-4A-10A plane	0.39 (1)	0.45	0.43 (2)	0.48
displacement of 13 from 1-2-3-4-4A-10A plane			0.09 (1)	0.08
4A-4-11	124.0 (3)	122.9	122.0 (3)	121.1
4-4A-4B	125.1 (14)	124.6	124.5 (2)	124.6
4-3-13			121.1 (5)	121.5
11···12	2.976 (6)	3.070	2.978 (4)	3.072
11···13			2.888 (11)	2.915

[a] Geometries were calculated with MMP2 and initial atomic coordinates from X-ray diffraction data. [b] Experimental numbers are average values obtained from both molecules in the asymmetric unit. [c] Dihedral angle about an imaginary 4···5 bond.

the 3,6-positions in **3** is to limit expansion of the interior angle (4A-4-11) between the interior methyl groups and the ring carbons to 122° as compared to 124° in **2**. This limitation requires a significant additional exaggeration of the twist in the ring system of **3**, to absorb unfavorable van der Waal's contact of the interior methyl groups as is apparent from the first four lines of Table III.

An additional feature of the geometries of **2** and **3** is the rotameric disposition of the methyl groups with respect to one another. In each case the methyl groups at the 4- and 5-positions have approximate C_2 symmetry with the hydrogens staggered or "geared" (conformation A). In both **2** and **3**, the interior methyl

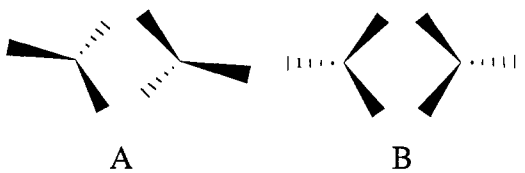

A B

groups adopt eclipsed conformations with their aromatic rings. In contrast adjacent methyl groups (3 and 4) in **3** exhibit σ

Table IV. Experimental and Calculated Heats of Formation, $\Delta H_f°$(g) (kcal/mol)

compd	exptl[a-c]	calcd[c]	difference[b]
1	48.2 ± 0.8 (49.5)	50.07 (49.08)	−1.87
2	46.3 ± 1.4	44.23 (40.16)	2.07
7	34.2 ± 0.6	33.69 (32.91)	0.51
3	38.3 ± 1.1 [33.7]	29.95	8.35 [3.75]
8	31.1 ± 0.9	27.74	3.36

[a] Data from ref 7 except value in parentheses. [b] Values in square brackets are calculated with the experimental $\Delta H_f°$(s)[7] and the calculated heat of sublimation. [c] Values in parentheses are from ref 5.

symmetry relative to each other with the hydrogens eclipsed (conformation B), which gives a quite reasonable H···H contact of 2.3 to 2.4 Å. (The X-ray determined H positions were altered to give a C–H distance of 1.11 Å for these calculations.)

Calculated Ground-State Geometries. The structures of **2** and **3** are reproduced reasonably well by MMP2 calculations with the 1982 force field.[14] Complete atomic coordinates for the calculated structures of **2** and **3** are given in the supplementary material. Bond distances in both structures are in very good to excellent agreement with the experimental values in the solid state. Moreover, the 4A–4–11 and 4–4A–4B bond angles also agree with the experimental values (Table III). The geared and eclipsed symmetries of the inner methyl groups of **2** and **3** and the adjacent methyl groups of **3** are also reproduced in the calculated structures. However, both structures are somewhat more distorted than the crystal geometries particularly with respect to the degree of twist in the ring system and the contact distances between the methyl groups (Table III). This result is not surprising given the tendency of aromatic rings in MMP2 to deform excessively to relieve strain.[21] All in all the calculated geometries are quite satisfactory.

Given the reasonable geometries calculated by MMP2 it is of interest to ascertain if ground-state strain energies of **2** and **3** and the corresponding buttressing effect can be calculated accurately. Experimental[7] and calculated heats of formation of the relevant compounds for this purpose are given in Table IV. With the outstanding exception of **3** the calculated heats of formation are in reasonable agreement with experimental values. As a consequence the calculated strain energy for the 4,5-methyl group interaction in **2** of 10.5 kcal/mol derived from **2** and **7** is close to the experimental value of 12.1 ± 1.5 kcal/mol.[7]

The reason for the large discrepancy in the calculated and experimental values of $\Delta H_f°$(g) for **3** is not entirely clear. It may derive in part from an underestimation of the steric energy of **3** by MMP2 due to excessive flexibility of the aromatic system. On the other hand, it is entirely possible that the experimental value derived from $\Delta H_f°(s) = \Delta H_f°(s) + \Delta H°_{sublimation}$ is incorrect. Although the calculated buttressing effect of the methyl groups at the 3,6-position of 2.2 kcal/mol (compare **3** and **8**) is far lower than the 7.2 ± 1.4 kcal/mol obtained from experimental values of $\Delta H_f°$(g), it is within experimental error of the solid-state strain energy [$\Delta H_f°$(s) for **3** − $\Delta H_f°$(s) for **8**] of 2.6 ± 1.1 kcal/mol.[7] Thus two-thirds of the experimental buttressing effect in $\Delta H_f°$(g) appears as a difference in the heats of sublimation or lattice energies of **3** (31.9 ± 0.9 kcal/mol) and **8** (27.3 ± 0.4 kcal/mol). In this regard it is interesting to note that the lattice energies of **2** and **7** are virtually identical and as a consequence the strain energies of **2** in the solid and vapor phase are within experimental error of one another.[7,22] It is therefore conceivable that the large experimental $\Delta H_f°$(g) and buttressing effect in **3** in the vapor phase may be due to an erroneously large heat of sublimation for **3**.

Given the crystal structures of **2** and **3** it is possible to calculate[16] the lattice energies of the molecules as a check of the original heats of sublimation. Although the calculated heat of sublimation for **2** of 25.9 kcal/mol is in good agreement with the reported experimental value, 25.0 ± 0.3 kcal/mol, the calculated value for **3** of 27.2 kcal/mol is substantially *lower* than the reported 31.9 kcal/mol and quite close to that for **8**. If, then, the experimental $\Delta H_f°$(g) for **3** is adjusted by using the heat of sublimation calculated from the crystal structure, the resulting $\Delta H_f°$(g) (Table IV) is in much closer agreement with the value obtained from force-field calculations. Furthermore, the "experimental" and calculated ground-state buttressing effects are now quite similar, being 2.6 and 2.2 kcal/mol, respectively.

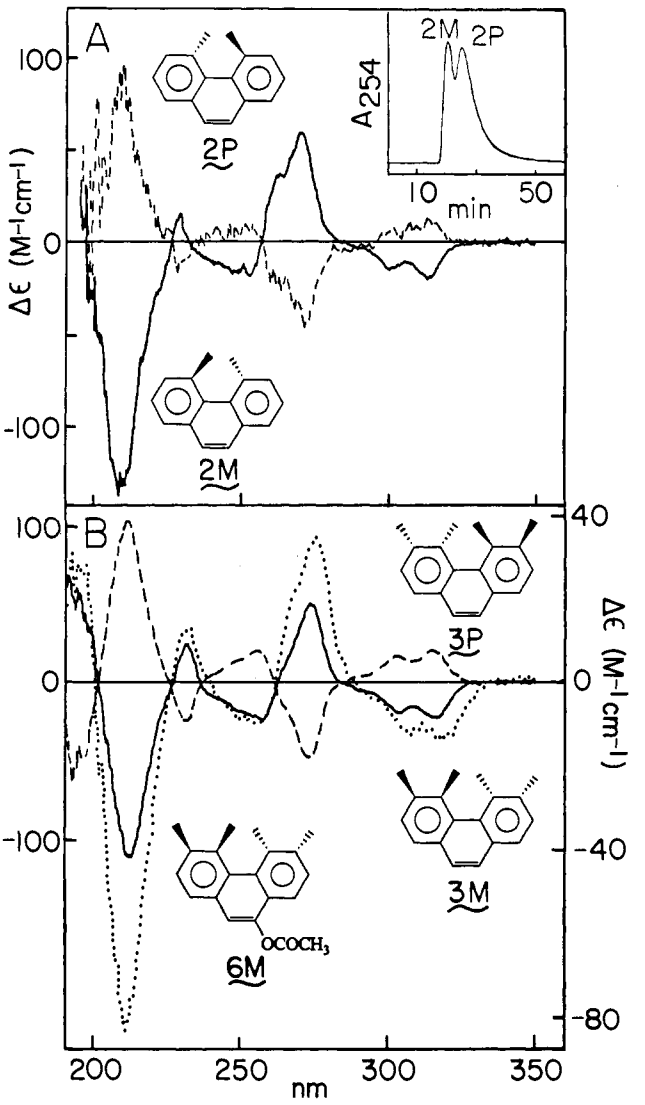

Figure 2. (A) Circular dichroism spectra of **2M** (—) and **2P** (---) at −60 °C obtained by cryogenic HPLC (inset) using (+)-poly(triphenylmethyl methacrylate) on silica at −78 °C. (B) Circular dichroism spectra of **3M** (—) and **3P** (---) at 0 °C and **6M** (···) at 25 °C. Scale on the right abscissa is for **6M**.

Isolation and Conformational Stability of the Antipodes of 2 and 3. Remarkably, the kinetically labile antipodes of **2** are separable by chromatography on (+)-poly(triphenylmethyl methacrylate) coated silica at cryogenic temperatures (−70 °C and below) as illustrated in Figure 2. The circular dichroism spectra of **2M** and **2P** at −60 °C can be used to assign the absolute configurations of conformers as discussed below. To the best of our knowledge this is the first direct observation of the conformational enantiomers of **2**.

The conformational antipodes of **3** are stable enough to be easily separated on chiral stationary phases at much more moderate temperatures.[11] The circular dichroism spectra of enantiomerically pure samples of **3M** and **3P** are illustrated in Figure 2. The absolute configuration of the two antipodes as well as those of **2** can be unambiguously assigned by stereoconservative preparation of **6M** from the corresponding *cis*-dihydrodiol of M configuration

(21) Allinger, N. L. *Quantum Chemistry Program Exchange*; Indiana University Chemistry Department, 1982; No. MMP2, p 7.1.

(22) A similar observation is made with respect to two isomeric dimethylbenz[*a*]anthracenes also compared in ref 7.

Table V. Experimental and Calculated Activation Parameters for Pseudorotations at 25 °C

compd	exptl $\Delta G^{\ddagger}$, kcal/mol	exptl $\Delta H^{\ddagger}$, kcal/mol	exptl $\Delta S^{\ddagger}$, eu	calcd $\Delta\Delta H_f°(g)$, kcal/mol
2	16.1 ± 1.5	13.9 ± 0.9	−7.3 ± 4.1	17.37 (20.00)[a]
3	23.1 ± 0.5 (22.9)[b]	21.9 ± 0.2	−3.9 ± 0.7	23.09
6	23.5 ± 0.4	22.3 ± 0.2	−4.1 ± 0.6	
4	(23.7)[c]			15.79
5[d]	18.1	17.9 ± 1.5	−0.5 ± 4.5	

[a] Value from ref 5. [b] Measured at 30 °C, ref 11. [c] Estimated from data in ref 2. [d] Values obtained from data in ref 10.

and comparison of its circular dichroism spectrum to those of the chiral hydrocarbons (Figure 2). In both cases the first eluting enantiomer is the one of M helicity.

Activation parameters determined for inversion of configuration of **2**, **3**, and related compounds are given in Table V. A buttressing effect ($\Delta G^{\ddagger}(\mathbf{3}) - \Delta G^{\ddagger}(\mathbf{2})$) for the methyl groups in the 3,6-positions of 7.0 ± 1.4 kcal/mol in the transition state for pseudorotation of **3** can be estimated from Table V. This is quite similar to the buttressing effect of 5.9 ± 0.7 kcal/mol measured for pseudorotation of *cis*-3,4,5,6-tetramethyl-9,10-dihydroxy-9,10-dihydrophenanthrene.[9,12]

Transition-State Structure for Pseudorotation of 2 and 3. In principle it is possible to use force-field calculations to predict both the size of the kinetic barrier and the molecular geometry of the transition states for pseudorotation of **2** and **3**. Structures of the transition states can be derived by forcing only a minimum restriction on their conformational freedom, the coplanarity of the 4- and 5-methyl groups, and the ring carbons to which they are attached, followed by energy minimization with MMP2.[14] One salient check of the veracity of the calculated structures of the transition states discussed below is to compute the activation energy for pseudorotation from the heats of formation of the ground and transition states. In both cases the calculated activation energies are within 1.3 kcal/mol or 10% of the experimental barriers (Table V). It should be pointed out that a recent calculation of $\Delta\Delta H_f°(g)$ between planar and twisted **2** with Allinger's 1985 force field gave a value of 16.75 kcal/mol.[23] The calculated buttressing effect in **3** is 5.7 kcal/mol.

Calculated transition-state structures for **2** and **3** are represented in Figure 3. Of particular interest is the degree of planarity of the transition states and the conformations of the methyl groups. The transition state for **2** has an essentially planar carbon framework with the methyl groups having σ symmetry (conformation B) relative to one another as opposed to the staggered conformation A of the ground state. The situation is similar for **3** except the structure shows significant deviation from planarity particularly with respect to the 3- and 6-methyl groups. In this instance the approximate relationship between adjacent methyl groups (3 and 4) changes from the eclipsed conformation A to staggered conformation B on going from the ground to the transition state. These observations clearly argue against a "gear"[24] or "cog-wheel" like coupled motion of methyl groups in the pseudorotation process and are consistent with the notion that the methyl group behaves as a symmetrical substituent,[25] or a "stripped gear". That the 3,6-methyl groups are out-of-plane with respect to the 4,5-methyl groups indicates that they may proceed or lag behind the inner methyl groups during pseudorotation.

Although it is clear that the interior methyl groups are closer together by about 0.15 Å and that the interior (4A–4–11) methyl-ring bond angles are expanded even further in the transition states for **2** and **3**, the most dramatic structural change is the exaggerated 4–4A–4B angle and the transmittal of the steric interaction across the ring resulting in the contraction of the

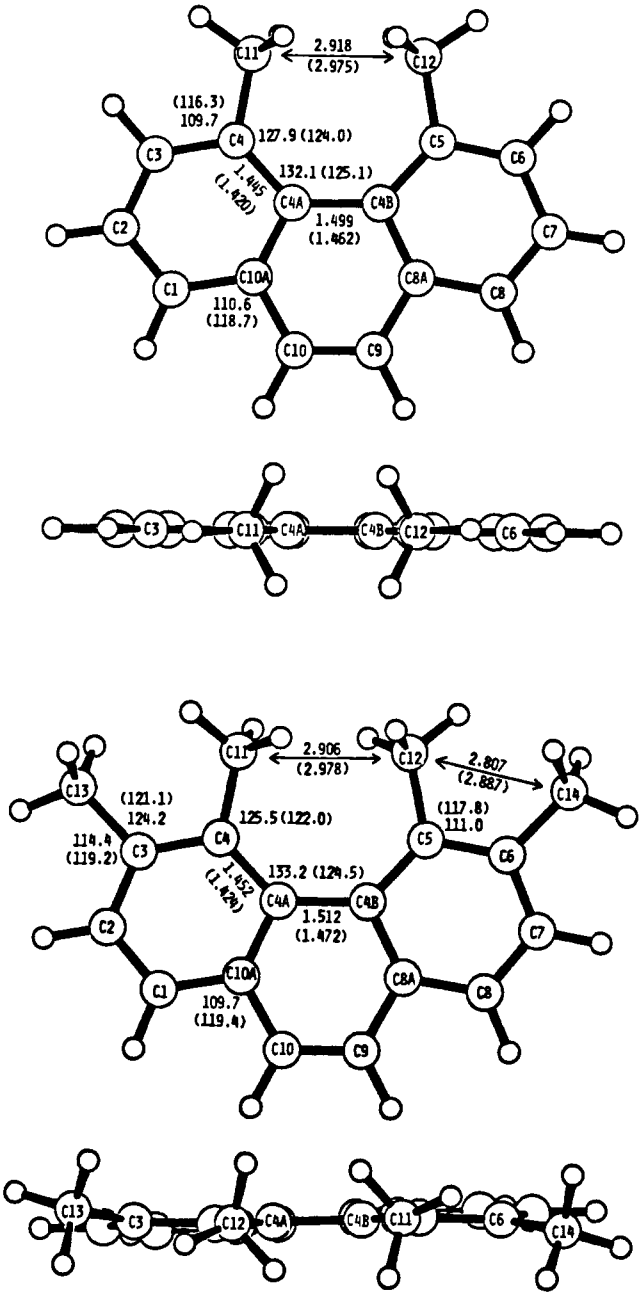

Figure 3. Transition-state geometries for pseudorotation of **2** (top) and **3** (bottom). Parameters in parentheses are those from the calculated ground-state structures. Atomic coordinates are given in the supplementary material.

8–8A–9 bond angle by 9 to 10°. The structural basis of the buttressing effect in pseudorotation of **3** is apparent from Figure 3. In short, the 3,6-methyl groups resist the severe van der Waal's repulsion between inner methyl groups by preventing the opening of the 4A–4–11 angle causing a further expansion or dimunition of the 4–4A–4B and 8–8A–9 angles, respectively, and a further lengthening of the 4A–4B bond. Another way to view the distortions of the phenanthrene skeleton in the transition state is as a 7 to 10° pivot of the outer rings about C8A and C10A away from the methyl–methyl interaction. Even though the transition-state geometries derived from these force-field calculations may be somewhat exaggerated,[21] they are at least reasonable and consistent with the available experimental facts.

It is clear that the conformational stability of **2** is considerably lower than has been previously thought.[2,10] The difference between the observed conformational stability of **4**[2] and the activation barriers for similar molecules such as **2** and **5**[10] (Table V) remains to be explained. Molecular mechanics calculations indicate **4**

(23) Sprague, J. T.; Tai, J. C.; Yuh, Y.; Allinger, N. L. *J. Comput. Chem.*, in press.
(24) Nilsson, B.; Martinson, P.; Olsson, K.; Cater, R. E. *J. Am. Chem. Soc.* **1974**, *96*, 3190.
(25) Charton, M.; Charton, B. *J. Am. Chem. Soc.* **1975**, *97*, 6472.

should be no more stable than **2**, suggesting that the conformational stability of **2** in solution has been overestimated.[2,10]

Finally, the experimental (or calculated) differences in ground-state strain energies of 2.6 kcal/mol (2.2 kcal/mol) and in activation energies of 7.0 kcal/mol (5.7 kcal/mol) for **2** and **3** provide estimates for the difference in the strain energies for the transition states of **2** and **3** of 9.6 kcal/mol (7.9 kcal/mol). Not surprisingly, the buttressing effect of the 3,6-methyl groups is considerably greater in the transition state than in the ground state.

Acknowledgment. This work was supported by NSF Grant DMB 84 13502 to R.N.A. R.N.A. is the recipient of a NIH Research Career Development Award (ES 00133). The authors are particularly grateful to Prof. M. S. Newman for his generous gift of the title compounds and Prof. N. L. Allinger for a copy of ref 23 prior to publication. Support by the National Science Foundation (CHE-84-02155) for purchase of the X-ray diffractometer is gratefully acknowledged. We thank Dr. D. M. Barnhart for assistance with the preliminary X-ray work on **3**.

Supplementary Material Available: Tables of U values, intramolecular distances and angles, atomic positional parameters, and atomic coordinates for **2** and **3** (17 pages); listing of structure factors (25 pages). Ordering information is given on any current masthead page.

A Concise and Stereoselective Route to the Predominant Stereochemical Pattern of the Tetrahydropyranoid Antibiotics: An Application to Indanomycin

Samuel J. Danishefsky,* Shari DeNinno, and Paul Lartey

Contribution from the Department of Chemistry, Yale University, New Haven, Connecticut 06511. *Received September 2, 1986*

Abstract: The reactions of (*E*)- and (*Z*)-crotylsilanes of the type $R_3Si—CH_2—CH=CH—CH_3$ with activated glycal derivatives in the presence of BF_3 etherate have been examined. In all cases, the reactions were regiospecific, resulting in incorporation of a 3-methylprop-1-ene-3-yl function at the 2-position of the pyran with formation of a 3,4 double bond. The reactions also demonstrate virtual facial specificity. The carbon nucleophile enters trans to the substituent at the 6-position, leading to a 2,6-anti relationship. The topographic selectivity which defines the relationship of the configuration of the *sec*-butenyl group relative to C_2 of the pyran is a function of several variables. The most significant of these is the stereochemistry (*E* or *Z*) of the crotyl group and the presence or absence of substitution at the 3-position of the pyran. Some sensitivity to the electronegativity of the activating group is also manifested. By combining the most favorable features for topographic selectivity, a highly concise and highly stereoselective (Zimmerman definition) construction of the primary pattern (1′-anti 2,6-trans) of the title compounds is achieved. A synthesis of the pyranoid segment of indanomycin in optically active form based on this chemistry is described.

I. Background

When the repertoire of extensively oxygenated natural products is examined, the widespread occurrence of the trialkylated tetrahydropyrans becomes apparent.[1] Compounds housing such substructures commonly exhibit significant ionophoric, antibacterial, or antifungal activity. The 2-position of the ring is often substituted with an isopropyl or a sec-butyl group, usually in oxidized form. The 6-position is generally connected to a longer chain which contains extensive oxygenation. There is usually a trans relationship between the substituents at positions 2 and 6 (see structures **1a** and **1b**).[2,3]

Another little noted connectivity involves the stereogenic centers at $C_{1'}$ of the side chain and at the 2-position of the pyran.[4] If the side chain $C_{1'}$–$C_{2'}$ bond is drawn antiperiplanar to the 2–3 bond of the ring, the branching substituent (usually methyl, occasionally ethyl) at $C_{1'}$ and the ring oxygen are anti (see structure **1a**).[2] Only rarely is the syn pattern (see structure **1b**) encountered.[3]

Scheme I

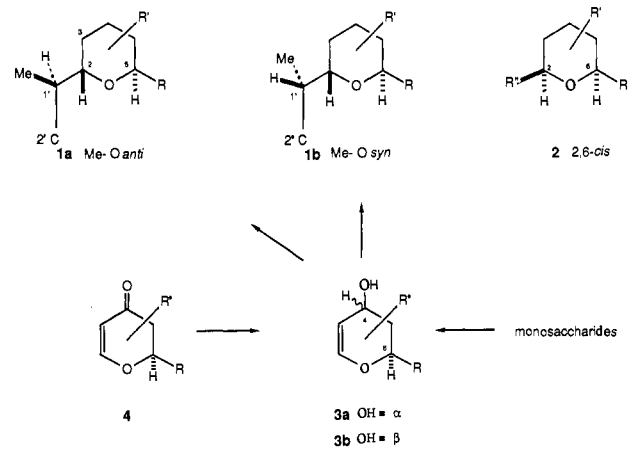

As part of a broader program directed toward the synthesis of highly oxygenated natural products, we focused on these substructural features. A particularly attractive solution would be one which exploited intermediates of the type **3**. Depending on the nature of R and R′, such intermediates might well be readily available via transformation of monosaccharides.[5a] An alternative

(1) For an extensive compilation of such compounds see: (a) Westley, J. W., Ed. *Polyether Antibiotics*; Marcel Dekker: New York, 1083; Vol. I and II. (b) For the structure of zincophorin see: Brooks, H. A.; Gardner, D.; Poyser, J. P.; King, T. J. *J. Antibiot.* **1984**, *37*, 1501.

(2) For instance, several compounds with the common 2,6-*trans*-1′-*anti* relationship, cf. inter alia, nigericin, salinomycin, narasin, lasalocid A, indanomycin (X-14547A), grisorixin,[1a] and zincophorin.[1b]

(3) Alborixin and X-206[1a] are examples of 2,6-cis ionophores. It is interesting to note that they also possess the 1′-syn relationship. A 1′-syn relationship in a more oxidized spiro ketal substrate is encountered in the avermectins.

(4) For consistency, the numbering system used throughout this paper is that of a pyran nucleus (oxygen is position 1). This system is maintained even for sugar derivatives.

0002-7863/87/1509-2082$01.50/0